JOURNAL OF MATERIALS SCIENCE 30 (1995) 3547–3551

Specific heat of the Hf_2Fe, Hf_2Co, and Hf_2Rh intermetallic compounds

N. IVANOVIĆ, D. RODIĆ*, B. CEKIĆ, M. MANASIJEVIĆ, S. KOIČKI, D. BABIĆ‡, R. NIKOLIĆ§
*Laboratory of Physics, *Laboratory of Theoretical and Solid State Physics, ‡Laboratory of Radiation Chemistry, and §Laboratory of Chemistry, P.O. Box 522, 11001 Belgrade, Yugoslavia*

The specific heat under constant pressure, C_p, of intermetallic compounds Hf_2Fe, Hf_2Co and Hf_2Rh with the Ti_2Ni structure was obtained by means of differential thermal analysis in the temperature range 275–740 K. The results differ significantly from the Debye theory, even when a correction for optical phonons in Einstein approximation is considered, which indicates existence of a defect contribution to the specific heat. Relative entropy has been determined and the obtained results were fitted and analysed. The anomalous temperature behaviour of C_p is discussed, having in mind results of previous investigations of these and similar systems, obtained by other methods.

1. Introduction

The relation between structure and electric-field gradient (EFG), as well as a high affinity toward hydrogen of hafnium intermetallic compounds have been recently extensively investigated [1–10]. Investigations of Hf_2Rh and Hf_2Co are in progress and will be published soon. The temperature dependence of the hydrogen content and absorption rate [2–4, 9] and preferential positions of absorption [10] have been determined. The preferential absorption at the first coordination around the 48*f* position, an absorption anomaly around 470 K, and changes of the electric-field gradient and magnetic properties during hydrogenization of Hf_2Fe, have been reported. As a consequence of these experimental results and the recent theoretical [11] and experimental [12] investigations, the hypothesis of a strong *d*–*d* hybridization in these compounds is established. However, the reported anomalies of EFG and hydrogen absorption temperature dependence in Hf_2Fe are not completely understood and the two other systems, Hf_2Co and Hf_2Rh have been poorly investigated so far.

2. Synthesis and crystal structure of the samples

The samples were prepared by melting stoichiometric quantities of 99.97% pure Hf, except for 2% Zr, and 99.98% pure Rh and Co, in a radio frequency (r.f.) inductive furnace. X-ray diffraction [1, 13] (a similar quality diffractogram for Hf_2Rh has also been obtained), and microprobe analyses [14] confirm that the obtained 5 g rods have Ti_2Ni structure, with the presence of about, or less than, 3% of other phases. Ti_2Ni structure has a face-centred cubic lattice with the F*d*3*m* space group and 96 atoms in the unit cell [1, 15, 16]. Hafnium atoms occupy two non-equivalent crystallographic positions 16*c* and 48*f* and iron, rhenium and cobalt occupy 32*e* position. A distance of about 0.1 nm between the first and the second coordination sphere around hafnium atoms at both crystallographic positions is reported [1]. Some of the materials parameters are presented in Table I.

3. Specific heat measurements

The specific heat measurements are performed using a Perkin–Elmer DSC-2 differential thermal analysis (DTA) system, in the temperature range between 275 and 740 K. Aluminium sample holders and a sapphire standard were used. The heating velocity was 10 or 20 K min^{-1}. Specific heat was evaluated from the equation

$$C_p = \frac{W_s D_s}{W D} C_{ps} \quad (1)$$

where W_s and W are masses, and D_s and D are obtained signals, of the sapphire standard and the sample, respectively. C_{ps} are tabulated specific heat values of the sapphire standard at corresponding temperatures. A correction was made for the aluminium holders mass difference. The base line was flat and stable during the measurements. The maximum error in the measurements was estimated to be about 3%.

4. Results

The results of the specific heat measurements of Hf_2Fe, Hf_2Co and Hf_2Rh with a 10 K min^{-1} scanning rate are presented in Fig. 1a–c, respectively.

0022–2461

TABLE I Some parameters of the compounds: A, molecular weight; T_m, melting temperature; ρ, density; H_{for}, energy of formation; a, lattice constant

Compound	A ($g\,mol^{-1}$)	T_m (K) [19]	ρ^a [$g\,cm^{-3}$]	H_{for} ($kJ\,mol^{-1}$) [20–22]	a (nm)
Hf_2Fe	412.8	1533	12.3	−23, −30[b]	1.2025
Hf_2Rh	459.9	1773	13.5	−95[b]	1.2271 [9]
Hf_2Co	415.4	1588	12.8	−38, −51[b]	1.2066

[a] Density obtained by Peltier method.
[b] Predicted values for HfFe, HfRh and HfCo.

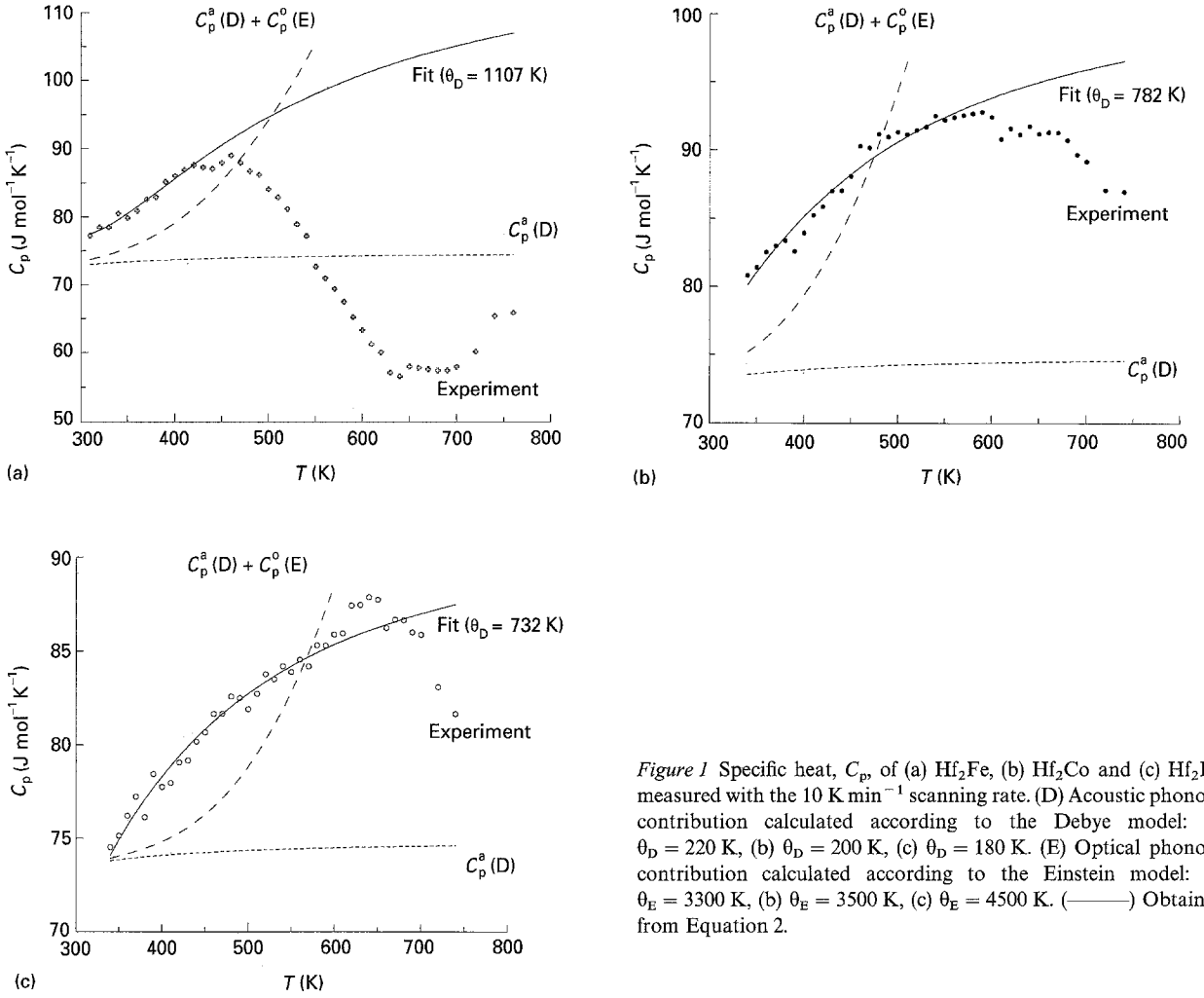

Figure 1 Specific heat, C_p, of (a) Hf_2Fe, (b) Hf_2Co and (c) Hf_2Rh measured with the 10 K min^{-1} scanning rate. (D) Acoustic phonons contribution calculated according to the Debye model: (a) θ_D = 220 K, (b) θ_D = 200 K, (c) θ_D = 180 K. (E) Optical phonons contribution calculated according to the Einstein model: (a) θ_E = 3300 K, (b) θ_E = 3500 K, (c) θ_E = 4500 K. (———) Obtained from Equation 2.

A pronounced drop of the Hf_2Fe specific heat starts around 470 K, and continues to approximately 650 K, and from about 700 K, $C_p(T)$ starts to increase again. Numerical derivation of the experimental data has been performed and anomalous points are found to be at 430 and 650 K. An additional discontinuity in experimental data around 560 K corresponds to the point of the maximum falling rate of $C_p(T)$ dependence. The drop in the Hf_2Co specific heat begins around 590 K and for Hf_2Rh around 640 K. The numerical procedure gives 560 and 620 K as anomalous points. Only the beginning of the Hf_2Co and Hf_2Rh anomaly can be observed in the measuring range of the equipment used.

The 20 K min^{-1} scanning rate results obtained for the three different Hf_2Fe samples, taken from the same rod, are presented in Fig. 2a–c. Anomalies are observed at 520, 550 and 480 K, respectively. The numerical procedure confirms the results. A good agreement of the results before and large discrepancies after the anomaly point are obvious. Starting points of the anomalous behaviour of all measured $C_p(T)$ dependences on T_c are presented in Table II.

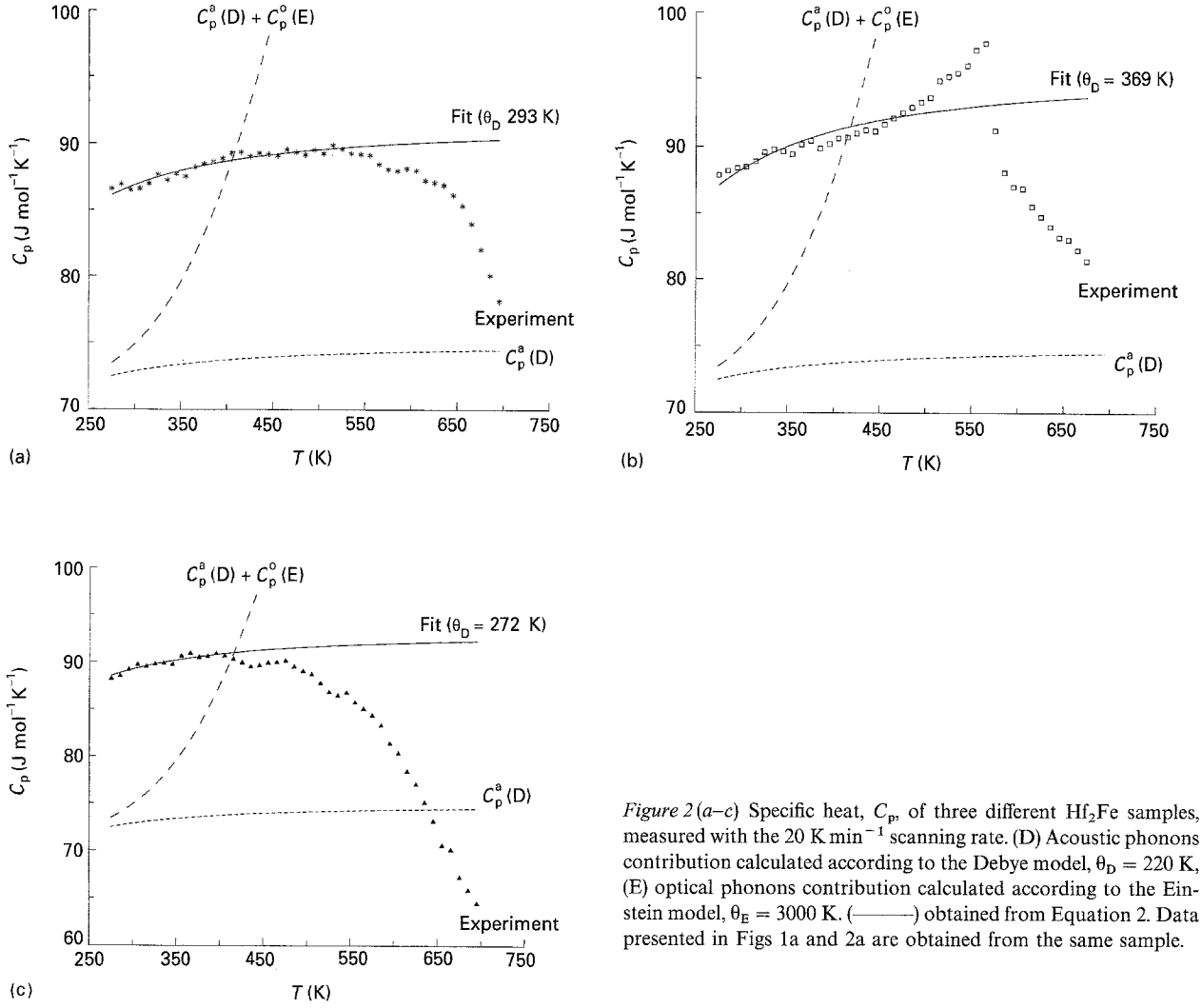

Figure 2 (a–c) Specific heat, C_p, of three different Hf_2Fe samples, measured with the 20 K min^{-1} scanning rate. (D) Acoustic phonons contribution calculated according to the Debye model, θ_D = 220 K, (E) optical phonons contribution calculated according to the Einstein model, θ_E = 3000 K. (———) obtained from Equation 2. Data presented in Figs 1a and 2a are obtained from the same sample.

TABLE II The results of the fitting procedure according to Equations 3 and 4, and numerically obtained starting points of the anomaly T_c

Compound	θ_D		Number of modes, $N \times 10^{-24}$ (θ_D fitted)	θ_E (fitted) (K)	T_c (K)
	(Fitted) (K)	(Estimated) (K)			
Hf_2Fe[a]	1107	220 [1]	2.87	3300	430
Hf_2Co[a]	782	200	2.46	3500	560
Hf_2Rh[a]	732	180 [24]	2.22	4500	620
Hf_2Fe (a)[b]	293	220 [1]	2.2	3000	520
Hf_2Fe (b)[b]	369	220 [1]	2.3	3000	550
Hf_2Fe (c)[b]	272	220 [1]	2.24	3000	450

[a] 10 K min^{-1} scanning rate.
[b] (a), (b), (c), 20 K min^{-1} scanning rate.

The first part of the $C_p(T)$ dependencies, far away from any anomaly, is fitted according to the equation [17]

$$C_p = 3Nk_B\left[1 - \frac{1}{20}\left(\frac{\theta_D}{T}\right)^2 + \frac{1}{560}\left(\frac{\theta_D}{T}\right)^4\right] \quad (2)$$

k_B is the Boltzmann constant and T the temperature (K). The total number of oscillating modes, N, and the Debye temperature, θ_D, have been taken as free parameters of the fit. In Figs 1 and 2, these fitted curves are presented by solid lines. The results obtained from the Debye theory

$$C_p^a = 3Nk_B\left[3\left(\frac{T}{\theta_D}\right)^3 \int_0^{\theta_D/T} x^4 \frac{e^x}{(e^x - 1)^2} dx\right] \quad (3)$$

are represented by dotted lines. The total number of modes, N, is considered to be $3N_a$ where N_a is the Avogadro number. The optical phonon

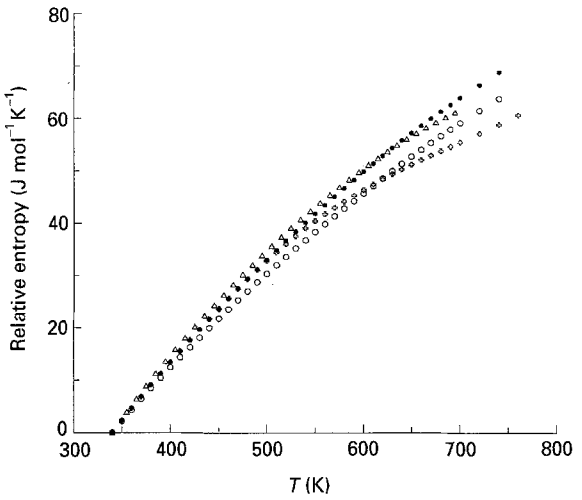

Figure 3 Calculated specific entropy of (✣,△) Hf_2Fe, (●) Hf_2Co and (○) Hf_2Rh. (✣) 10 K min^{-1}, (△) 20 K min^{-1}.

contribution is accounted for in the Einstein approximation [18]

$$C_p^o = 3Nk_B\left[(3s - 3)\, y^2 \frac{e^y}{(e^y - 1)^2}\right] \quad (4)$$

where s is the number of atoms in the primitive cell, $y = \theta_E/T$, θ_E is the Einstein temperature. The corrected curve is presented by the dashed line (short dashes). The results of calculations are presented in Table II.

The calculated temperature dependence of relative entropy is presented in Fig. 3.

5. Discussion

The most interesting detail of the $C_p(T)$ dependencies is the pronounced saddle points at approximately 430, 560 and 620 K for Hf_2Fe, Hf_2Co and Hf_2Rh, respectively. The characteristic shape, large transition temperature interval (430–650 K for Hf_2Fe) and entropy data (Fig. 3) indicate a diffuse-phase transition of the second order. Differences between $C_p(T)$ dependencies of the same sample obtained with different scanning rates should be attributed to the transition dynamics. The 20 K min^{-1} scanning rate compresses the transition into a smaller temperature interval, shifting the starting point of the anomaly towards the temperature of the maximum falling rate of the 10 K min^{-1} characteristic. Differences in the transition shape and dynamics are clearly observed for the 20 K min^{-1} $C_p(T)$ curves of the three different samples of Hf_2Fe, though the data below the transition are in good agreement. This might be connected to the diffuse nature of the transition. Calculations from Equation 3 show that the Debye theory considerably underestimates the experimental results. An acceptable fit using this theory can be achieved only when both the Debye temperature, θ_D, and number of oscillating modes, N, have very high values. Moreover, correction for optical phonon contribution (Equation 4) does not improve the fit sufficiently to match the experimental data, so an additional (defect, rather than impurity) contribution to C_p should be considered. A comparison between Peltier and X-ray diffraction density [1] indicates the existence of a free volume space in the measured Hf_2Fe samples, which could explain at least differences in the anomalies' shape between these samples.

The position of the $C_p(T)$ anomalous point in Hf_2Fe is in a good agreement with the anomaly in TDPAC EFG [7, 8, 12] and hydrogen absorption measurements [2]. According to the TDPAC investigations [12], it seems that the phase transition should be attributed mainly to the 16*c* position (re)arrangement, while the 48*f* (and probably 32*e* position) remains quite stable. It is also observed ([12] and our preliminary TDPAC investigations of Hf_2Co and Hf_2Rh), that the weaker the EFG and the greater is its distribution, δ, the lower is the transition temperature of the corresponding compound ($Hf_2Fe < Hf_2Co < Hf_2Rh$). The same relation between melting temperatures, T_m [19], and predicted energies of formation, H_{for} [20–22], parameters strongly dependent on the *d–d* overlapping integral, is noticed (Table I). This indicates that the transition should be connected with specific electronic arrangements of *d* bands and the hybrid bonds formed by them.

Saturation of the magnetic moment at the hydrogen concentration of about 3 H atoms per molecule of Hf_2Fe [2], local concentrations of hafnium and iron, cobalt and rhenium in the first coordination around stable 48*f* and 32*e* positions [1], and the refinement calculations of X-ray diffractions data for the annealed and unannealed Hf_2Co sample [13], indicate that, in these compounds, the specific distribution of hybrid bonds prefers local configurations with a concentration of about 3 Hf atoms on 1 Fe. At the first coordination, around the 16*c* position, the ratio of hafnium and iron (cobalt, rhenium) is 1:1, and the condition is far from being fulfilled, so this configuration might be inherently unstable and its formation enabled by the

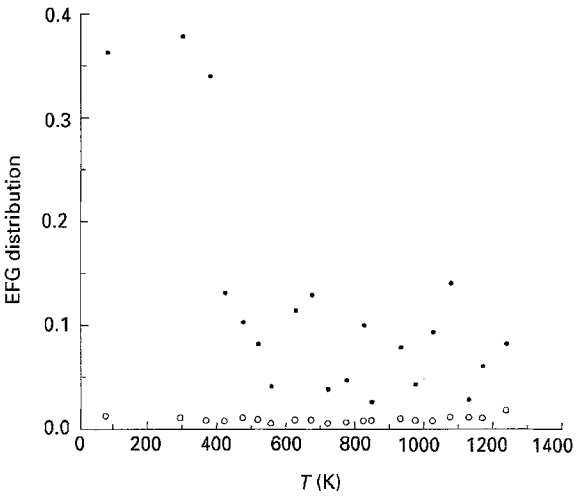

Figure 4 Temperature dependence of the EFG distribution parameter obtained at (●) 16*c* and (○) 48*f* crystallographic positions in Hf_2Fe, by TDPAC. The relative error of the 16*c* data is about 40% below and 25% above the anomaly point. The relative error of the 48*f* data is about 10% over the entire temperature range.

Ti_2Ni structure ordering. Consequently, some kind of relaxation at the 16*c* position, above a certain temperature, through the (re)organization of the hybrid bonds, could be expected. The difference between the magnitude and temperature behaviour of the EFG distribution parameter, δ, at 16*c* and 48*f* positions in Hf_2Fe obtained by TDPAC measurements (Fig. 4) is in a good agreement with this hypothesis.

6. Conclusion

The specific heat of intermetallic compounds with Ti_2Ni structure, Hf_2Fe, Hf_2Co and Hf_2Rh, exhibits several interesting features in the temperature range between 275 and 740 K. The most remarkable one is a pronounced saddle point at 430 (Hf_2Fe), 560 (Hf_2Co) and 620 K (Hf_2Rh), which is probably a characteristic of a diffuse phase transition of the second order. Some considerations (Fig. 4, [7, 8, 10, 12]) indicate that this phase transition should be attributed mainly to the 16*c* crystallographic position (re)organization.

Differences between the results obtained with $10\,K\,min^{-1}$ and $20\,K\,min^{-1}$ scanning rate over the entire measured temperature range are caused by a great sensitivity of the phase transition dynamic on the scanning rate, e.g. the sample heating rate. Differences between the data obtained for different Hf_2Fe samples with $20\,K\,min^{-1}$ scanning rate after the anomalous point, could be explained by the diffuse nature of the transition.

It is also obvious (Figs 1 and 2) that neither the Debye theory nor its correction for optical phonons, could fit the experimental data in a satisfactory way in the region below the transition. However, the general trend of the data obtained with the $20\,K\,min^{-1}$ scanning rate are in a better agreement with the pure Debye model, and the $10\,K\,min^{-1}$ one, with the corrected curve. In both cases, theory underestimates the number of oscillating modes, but the lower scanning rate furnishes more information about their origin. The rest of the mismatch between theory and the experiment should be attributed to a defect contribution, arising preferentially around the 16*c* position.

The microscopic nature of the investigated phenomena has not been completely elucidated. It is, by all means, connected with the characteristics of the *d–d* hybridization taking place in these compounds. Some experimental observations [12, 23], melting temperatures [19], predicted energy of formation [20–22], and theoretical predictions made for somewhat different systems [11], indicates that the *d*-band structure (precisely, the number and peculiarities of antibonding states in formed *d–d* bonds) has a great influence on formation, structure, and stability of the crystallographic positions in these compounds.

References

1. B. CEKIĆ, B. PRELESNIK, S. KOIČKI, D. RODIĆ, M. MANASIJEVIĆ and N. IVANOVIĆ, J. *Less-Common Metals* **171** (1991) 9.
2. P. VULLIET, G. TEISSERON, J. L. ODDOU, C. JEANDEY and A. YAOUANC, *ibid.* **104** (1984) 13.
3. G. TEISSERON, P. VULLIET and L. SCHLAPBACH, *ibid.* **130** (1987) 163.
4. K. H. J. BUSCHOW and A. M. VAN DIEPEN, *Solid State Commun.* **31** (1979) 469.
5. B. CEKIĆ, S. KOIČKI, M. MANASIJEVIĆ and B. PRELESNIK, *Hyperf. Interact.* **39** (1988) 303.
6. L. G. SHPINKOVA, A. A. SOROKIN, G. K. RYASNIYI, L. N. KRYUKOVA, B. A. KOMISSAROVA and Z. Z. AKSELYROD, *Izvest. Akad. Nauk SSSR Ser. Fiz.* **52** (1988) 1749.
7. Z. Z. AKSELROD, B. A. KOMISSAROVA, L. N. KRYUKOVA, G. K. RYASNYI, L. G. SPHINKOVA and A. A. SOROKIN, *Phys. Status Solidi (b)* **160** (1990) 255.
8. B. CEKIĆ, S. KOIČKI, N. IVANOVIĆ and M. MANASIJEVIĆ, *Izvest. Akad. Nauk Rossii, Ser. Fiz.* **56** (1992) 206.
9. R. M. VAN ESSEN and K. H. J. BUSCHOW, *J. Less-Common Metals* **64** (1979) 277.
10. J. L. SOUBEYROUX, D. FRUCHART, S. DERDOUR, P. VULLIET and A. ROUALT, *ibid.* **129** (1987) 187.
11. P. H. DEDERICH, B. DRITTLER, R. ZELLER, H. EBERT and W. WEINERT, *Hyperf. Interact.* **60** (1990) 547.
12. S. KOIČKI, B. CEKIĆ, N. IVANOVIĆ, M. MANASIJEVIĆ and D. BABIĆ, *Phys. Rev. B.* **48** (1993) in press.
13. B. CEKIĆ, D. RODIĆ, N. IVANOVIĆ, M. MITRIĆ, S. KOIČKI and M. MANASIJEVIĆ, in "Book of Abstracts of the XIII Yugoslav Conference on Condensed Matter Physics", Vranje, Yugoslavia, 28–30 September 1993, p. 88. "*Annal. Matica Srpska* (1993), in press.
14. N. IVANOVIĆ, M. SREĆKOVIC, A. MILOSAVLJEVIĆ, B. CEKIĆ, M. MANASIJEVIĆ, N. POPOVIĆ, N, BACKOVIĆ, M. DJURIĆ, A. KUNOSIĆ, K. NEMEŠ, G. ČOGURIĆ and U. MIOČ, *Infrared Phys.* (1993) to be published.
15. G. A. YURKO, J. W. BARTON and J. GORDON PARR, *Acta Crystallogr.* **12** (1959) 909. *Struct. Rep.* **23** (1959) 195.
16. *Idem,*
17. DZH. MAYER and M. GEPPERT-MAYER, in "Satistiheskaya Mehanika" (Mir, Moscow, 1980) p. 388.
18. I. LICEA, A. IOANID and A. DAFINEI, *Phys. Status Solidi (a)* **118** (1990) 131.
19. W. G. MOFFAT, in "The Handbook of Binary Phase Diagrams" (Genium, Schenectady, 1984).
20. R. BOOM, F. R. DeBOER, A. K. NIESSEN and A. R. MIEDEMA, *Phys. B* **115** (1983) 285.
21. A. K. NIESSEN, A. R. MIEDEMA, F. R. DeBOER and R. BOOM, *ibid.* **151** (1988) 401.
22. A. R. MIEDEMA, *Philips Tech. Rev.* **36** (1976) 217.
23. N. IVANOVIĆ, B. ANTIĆ, B. CEKIĆ, D. RODIĆ, M. MANASIJEVIĆ and S. KOIČKI, in "XXXVI Yugoslav Conference ETAN", Belgrade, Yugoslavia, 20–23 September 1993.
24. R. KUENTZLER and R. M. WATERSTRAT, *Solid State Commun.* **68** (1988) 85.

Received 22 October 1993
and accepted 27 July 1994